



Bacterial cell-surface displaying of thermo-tolerant glutamate dehydrogenase and its application in L-glutamate assay

Jianxia Song^{a,b,1}, Bo Liang^{b,1}, Dongfei Han^{b,1}, Xiangjiang Tang^b, Qiaolin Lang^b, Ruirui Feng^a, Lihui Han^{a,**}, Aihua Liu^{b,*}

^a Key Laboratory of Marine Chemistry Theory and Technology of Ministry of Education, and College of Chemistry and Chemical Engineering, Ocean University of China, 238 Songling Road, Qingdao 266100, China

^b Laboratory for Biosensing, and Key Laboratory of Biofuels, Qingdao Institute of Bioenergy & Bioprocess Technology, Chinese Academy of Sciences, 189 Songling Road, Qingdao 266101, China

ARTICLE INFO

Article history:

Received 24 August 2014

Received in revised form 1 December 2014

Accepted 2 December 2014

Available online 29 December 2014

Keywords:

Bacterial surface display

L-Glutamate

Thermo-tolerant glutamate dehydrogenase

Enzyme inhibition

L-Glutamate detection

ABSTRACT

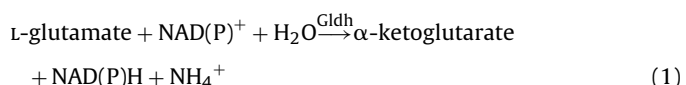
In this paper, glutamate dehydrogenase (Gldh) is reported to efficiently display on *Escherichia coli* cell surface by using N-terminal region of ice the nucleation protein as an anchoring motif. The presence of Gldh was confirmed by SDS-PAGE and enzyme activity assay. Gldh was detected mainly in the outer membrane fraction, suggesting that the Gldh was displayed on the bacterial cell surface. The optimal temperature and pH for the bacteria cell-surface displayed Gldh (bacteria-Gldh) were 70 °C and 9.0, respectively. Additionally, the fusion protein retained almost 100% of its initial enzymatic activity after 1 month incubation at 4 °C. Transition metal ions could inhibit the enzyme activity to different extents, while common anions had little adverse effect on enzyme activity. Importantly, the displayed Gldh is most specific to L-glutamate reported so far. The bacterial Gldh was enabled to catalyze oxidation of L-glutamate with NADP⁺ as cofactor, and the resultant NADPH can be detected spectrometrically at 340 nm. The bacterial-Gldh based L-glutamate assay was established, where the absorbance at 340 nm increased linearly with the increasing L-glutamate concentration within the range of 10–400 μM. Further, the proposed approach was successfully applied to measure L-glutamate in real samples.

© 2014 Elsevier Inc. All rights reserved.

1. Introduction

Glutamate dehydrogenase (Gldh) (EC 1.4.1.2–1.4.1.4), composed of 400–500 amino acids, is a widely existing enzyme in almost all living organisms [1], which can catalyze the reversible oxidative deamination of L-glutamate to α-ketoglutarate and ammonia in cells, typically shown in Eq. (1). Gldh plays a key role in catabolism of glutamic acid [2]. As a cofactor-dependent enzyme, Gldh can be divided into three types: NAD⁺ specific dependency (E.C. 1.4.1.2), NADP⁺ specific dependency (E.C. 1.4.1.4) as well as

both NAD⁺ and NADP⁺ dependency (E.C. 1.4.1.3) [1].



As the primary excitatory neurotransmitter, glutamate is involved in some basic activities including learning and memory in the central nervous system [3]. Glutamate in abnormal concentration can induce disorders such as epilepsy, amyotrophic lateral sclerosis or Parkinson's disease and other neurological diseases. As one of the basic amino acids of nitrogen metabolism in body, glutamate has great significance on the metabolism, which is not only the intermediate metabolite of the tricarboxylic acid cycle [4], but also the element source of purine base and pyrimidine. Glutamic acid is also the main composition of protein widespread in nature. Additionally, glutamate is well known as monosodium glutamate (MSG), which is commonly used as a flavor in conjunction with other food additives in most food processing. However, the excessive intake of MSG can bring about several neurological disorders, such as excitotoxicity, stroke, epilepsy, and Alzheimer's disease

* Corresponding author at: Laboratory for Biosensing, and Key Laboratory of Biofuels, Qingdao Institute of Bioenergy & Bioprocess Technology, Chinese Academy of Sciences, 189 Songling Road, Qingdao 266101, China. Tel.: +86 532 80662758; fax: +86 532 80662778.

** Corresponding author at: Key Laboratory of Marine Chemistry Theory and Technology of Ministry of Education, Ocean University of China, 238 Songling Road, Qingdao 266100, China.

E-mail addresses: lhhan@ouc.edu.cn (L. Han), liuah@qibebt.ac.cn (A. Liu).

1 These authors contributed equally to this work.

[5–7]. Therefore, concerns about the safety of MSG were attracted around the world. Therefore, a rapid and effective analytical technique to evaluate glutamate level is highly desirable to avoid these disorders. To date, different approaches had been used to measure the concentration of glutamate, including microdialysis [8], capillary electrophoresis [9], fluorometry [10], high-performance liquid chromatography [11–14] and spectrophotometry [15], however, they either experienced complicated in procedure, or lacked of sensitivity and selectivity. Very recently, novel electrochemical glutamate biosensors based on nanoparticles functionalized with the glutamate oxidase (Glox) [16–18] or Gldh [19] have been developed for the sensitive detection of glutamate; nevertheless, the modification of the electrodes was complicated. Therefore, novel strategy is urgently needed for detection of glutamate.

The bacterial cell surface display provides an effective way in enzyme engineering. Enzyme-expressed cell can be reused without losing its activity and stability, which is cost-saving and convenient in comparison with using soluble free enzyme. To date, many types of anchoring motifs had been developed to intermediate the bacterial surface display of heterologous proteins [20,21], such as ice nucleation protein (INP), EstA from *Pseudomonas aeruginosa*, α -agglutinin, FadL and outer membrane protein C from *Escherichia coli* (*E. coli*) [22–26]. Although so many anchoring motifs can be used there, they have different effects on the host cells. So it is important to choose a suitable anchoring motif for an efficient, stable and special display of the fusion proteins. As an outer membrane protein, INP containing N-terminal and C-terminal domain was widely used to display target protein on the host cell surface, and the host cells can interact with substrates directly. So far, xylose dehydrogenase-, glucose dehydrogenase-, organophosphorus hydrolase-, xylanase-display systems and other surface display systems had been used to produce the target protein outside the cell membrane by cultivation, induction and centrifugation of recombinant *E. coli* strains [27–31]. The surface-display-based biosensing [30,32–34] as well as efficient biofuel cell [35,36] applications were realized. In the present study, a surface display system for the expression of Gldh from *Thermococcus waiotapuensis* [37] on the surface of *E. coli* with the truncated INP from *Pseudomonas borealis* as anchoring motif was developed. The activity, stability and substrate specificity of the displayed enzyme and effects of various ions on the enzyme activity of the displayed target protein were investigated. And finally, the freshly prepared whole-cell biocatalyst was applied for sensitive, selective and rapid detection of L-glutamate. To the best of authors' knowledge, this is the first report on the bacterial cell surface displaying specific Gldh (bacteria-Gldh) for optical determination of L-glutamate.

2. Materials and methods

2.1. Bacterial strain, plasmid, and culture conditions

In this study, pET28a (+) was used as the parent vector for the expression of INP-Gldh. *E. coli* DH5 α (F $^+$ φ 80 lacZΔM15Δ (lacZYA-argF) U169 endA1 recA1 hsdR17 (r_k^- , m_k^+) supE44λ-thi-1 gyrA96 relA1phoA) and *E. coli* strain BL21 (DE3) (F $^+$ ompT hsdS $_B$ (F $_B$ m_B^-) gal dcm (DE3)) were used as hosts for plasmid construction and expression of fusion protein, respectively. *E. coli* strains were grown in LB media with kanamycin (30 μ g/ml) or ampicillin (100 μ g/ml) at 37 °C and incubated by rotary shaking at 200 rpm. For the expression of INP-Gldh, strains were induced with isopropyl-β-D-thiogalactopyranoside (IPTG) at final concentrations ranging from 0.1 mM to 1 mM at 25 °C for 24 h when bacteria were grown to an OD₆₀₀ value within 0.4–0.6.

2.2. Construction of INP-Gldh

The wild type Gldh encoding gene was originating from the genome of *T. waio-tapuensis*, which was kindly gifted by Dr. Robb (Center of Marine Biotechnology, University of Maryland Biotechnology Institute, USA). The gldh gene was amplified by PCR under thermal conditions @ 94 °C for 30 s, 55 °C for 30 s, and 72 °C for 2 min, for each case lasting 35 cycles. Forward and reverse primers of polymerase chain reaction were 5'-CGCGGATCCATGGTTGAACCTGACCCGGTTGAAATGG-3' and

5'-CCCAAGCTTCAGTGACCCATCCGGG-3', respectively, with BamHI and HindIII as restriction sites (underlined). The amplified and purified PCR products were transferred into the pMD18-T vector, and then the gene after TA-cloning was digested with BamHI and HindIII restriction enzymes at the corresponding sites. And then it was inserted into the same sites of vector pTInaPb-N, which had been constructed using pET-28a (+) and N-terminal domain of INP in our lab [29]. The resultant plasmid was named as pTInaPb-N-Gldh, which was further transformed into *E. coli* BL21 (DE3) for the expression of fusion protein.

2.3. SDS-PAGE analysis and cell fractionations

E. coli strains harboring the expression of vector pTInaPb-N-Gldh were harvested after induction for 24 h. Then each fraction (outer membrane, inner membrane, and cytoplasm) of the cells was obtained by sonication and ultracentrifugation [29]. The membrane fractions were suspended in 100 mM Tris-HCl buffer (pH 8.0) for further analysis. Proteins in the whole cell lysates and subcellular fractions were analyzed by 12% (wt/vol) sodium dodecyl sulfate-polyacrylamide gel electrophoresis (SDS-PAGE) to detect the distribution of target protein. Culture without IPTG induction was used as a negative control.

2.4. Gldh activity assay

The induced cells harboring pTInaPb-N-Gldh were harvested by centrifugation and washed three times. Finally, the harvested cells were resuspended in 100 mM Tris-HCl buffer (pH 8.0). To measure the activity of Gldh, the absorbance at 340 nm representing production of NADPH (the reduced form of nicotinamide adenine dinucleotide phosphate) was recorded because Gldh can catalyze the reversible oxidative deamination of glutamate with NAD $^+$ as cofactor. The standard reaction system contained cells (OD₆₀₀ = 1.0), 2 mM L-glutamate and 0.5 mM NAD $^+$. The reaction was conducted at 60 °C for 2 min in a plastic tube and then centrifuged at 12,000 rpm for 1 min to terminate reaction. One unit of enzyme activity is defined as 1 μ mol NADPH generated per minute per entire OD₆₀₀ cell.

2.5. Effects of temperature and pH on enzyme activity

To investigate effects of temperature and pH on enzymatic activity of INP-Gldh, strains harboring recombinant plasmid were suspended in solutions varying pH at different temperatures. INP-Gldh activity in 100 mM Tris-HCl buffer (pH 8.0) was determined by spectrophotometer at temperatures ranging from 20 °C to 100 °C. The optimal pH tests were conducted at 60 °C using the following 100 mM buffers: sodium acetate (pH 5–6), potassium phosphate monobasic (pH 6–8), Tris-HCl (pH 7–9), glycine-NaOH (pH 9–10), and sodium carbonate-sodium bicarbonate (pH 10–11).

2.6. Effects of temperature and pH on enzyme stability

The harvested cells were suspended in 100 mM Tris-HCl buffer (pH 8.0) to investigate the stability of Gldh-displayed strain. The thermal stability was detected by incubating *E. coli* cells in 100 mM Tris-HCl buffer (pH 8.0) at temperatures within the range of 50–100 °C, and activity was measured hourly. The storage stability of recommended cells was determined by incubating them at different temperatures (4 °C, 25 °C, 37 °C and 60 °C) for 1 month, and Gldh activity was detected by taking out the same amount of sample solution for experiment at regular intervals. The pH stability of Gldh was investigated hourly by incubating equal volumes of cells in different buffer (pH 3–10.5) at 4 °C.

2.7. Substrate specificity assay

To study substrate specificity of the cell surface displayed Gldh for oxidative deamination of various α -amino acids, other amino acids instead of L-glutamate were used as substrate separately in the standard reaction system with a final concentration of 2 mM. Then the absorbance at 340 nm was recorded for comparison.

2.8. Effects of various ions on the enzyme activity

Different ions at a final concentration of 1 mM or 10 mM or 100 mM were mixed with enzyme-displaying recombinant cells separately, then enzyme activity was detected according to the standard reaction condition after incubation at 4 °C for 30 min. The relative response is defined as the ratio of the Gldh activity in the presence of each ion to the Gldh activity in the absence of ion.

2.9. L-glutamate detection using cell-surface expressed Gldh

Experiment conditions including the temperature, pH and time had been optimized in the previous studies. The absorbances at 340 nm are recorded varying with L-glutamate concentrations. For real sample measurement, the samples need to be successively pretreated, filtered and diluted using Tris-HCl buffer (pH 8.0) before detection. UV-vis absorption spectra ranging from 300 nm to 400 nm were measured after stopping reaction by removing the cells. All the experiments were repeated at least three times.

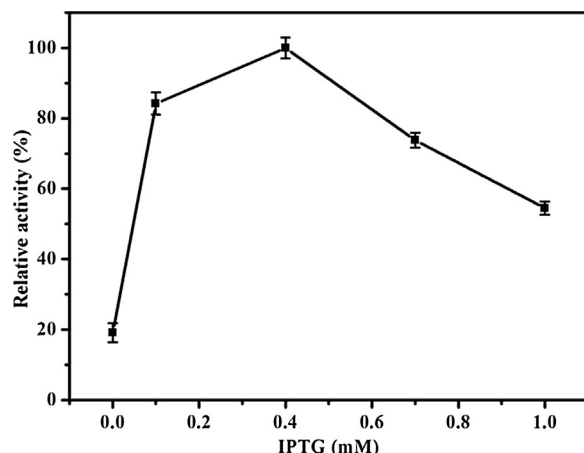


Fig. 1. Gldh activity of *E. coli* harboring expression vectors which were induced under different concentrations of IPTG.

3. Results and discussion

3.1. Construction of expression plasmids and the display of the fusion protein

The recombinant plasmid pTInaPb-N-Gldh was constructed successfully based on N-terminus gene of INP and pET28a (+) for the expression of Gldh on the cell surface of *E. coli*. Subsequently the recombinant plasmid was transformed into *E. coli* BL21 (DE3). Cells were harvested after induction for 24 h with IPTG. Various concentrations of IPTG were added into the culture to study the effect of IPTG on activity of recombinant protein. A highest enzyme activity was obtained when strains harboring plasmid pTInaPb-N-Gldh were cultured with 0.4 mM IPTG at 25 °C (Fig. 1), indicating that the appropriate concentration of IPTG realized a high expression of INP-Gldh and avoided the formation of inclusion bodies. In our initial experiments, *gldh* gene from *Bacillus subtilis* had been used to construct Gldh display system. However, it was expressed in the form of inclusion body at any IPTG concentration, suggesting that *gldh* gene from *B. subtilis* was incapable of achieving expression in soluble form in *E. coli* cells.

3.2. Cell fractionation and SDS-PAGE analysis

To investigate whether Gldh was expressed successfully on the surface of cells, whole cell lysates and cellular fractions of inner membrane of the recombinant *E. coli* were separated by sonication and centrifugation to collect the Gldh for SDS-PAGE analysis. Bands of about 60 kDa corresponding to INP-Gldh, which were found mostly in outer membrane fraction and a very small amount in cytoplasmic fraction of *E. coli* cells were used for expression. Meanwhile, no INP-Gldh fusion protein was detected there in the inner membrane fraction and any other fractions of the negative control strains (Fig. 2). This result indicated the successful construction of InaPb-N-Gldh plasmid and the correct location of fusion protein.

3.3. Enzyme activity of surface displayed Gldh

The Gldh activities of both the whole cells and cell fractions were measured, which are summarized in Table 1. Enzyme activity for the outer membrane fraction from *E. coli* harboring plasmid pTInaPb-N-Gldh was 17.96 ± 0.69 U/mg cells (3.12 ± 0.12 U/OD₆₀₀), accounting for approximately 90% of the whole cells activity. By contrast, there was little Gldh activity existed in the inner membrane fraction for the Gldh surface displaying cell and any fractions of the negative control strains. All the above results demonstrated

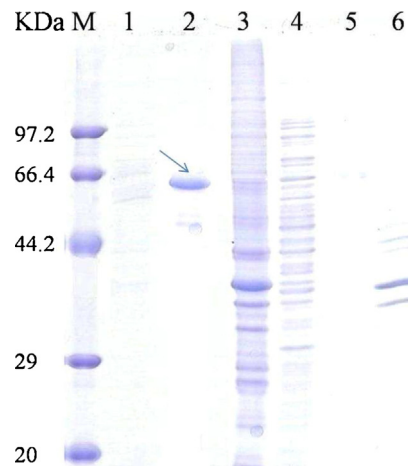


Fig. 2. Analysis of INP-Gldh protein from different cellular fractions by SDS-PAGE. Lane M, protein standard markers. Lanes 1–3, *E. coli* cells harboring pTInaPb-Gldh: lane 1, inner membrane fraction; lane 2, outer membrane fraction; lane 3, cytoplasmic fraction; lanes 4–6, the control strain: lane 4, cytoplasmic fraction; lane 5, inner membrane fraction; lane 6, outer membrane fraction.

that the INP-Gldh protein was properly displayed on the cell surface.

3.4. The effects of temperature and pH on INP-Gldh activity

The effects of temperature and pH on enzyme activity of INP-Gldh were studied (Fig. 3). The activity of bacteria-Gldh rose with the increasing temperature from 23 °C to 70 °C, and thereafter, the activity began to decrease (Fig. 3A), which may be caused by the instability of NADP⁺ [38]. It was found that the highest activity for Gldh occurred at 70 °C, which was higher than those for the purified free Gldh from *E. coli* (60 °C) and for Gldh from *Corynebacterium callunae* (30 °C) [39,40]. As shown in Fig. 3B, the whole cell could retain over 50% of its initial activity within the range of pH 7–10, however, the Gldh activity declined dramatically when the pH was lower than 7.5 or higher than 9.5. The optimal pH value was around 9.0 for bacteria-Gldh, which was similar with other hyperthermophilic Gdhs. It was reported that the optimal pHs for the oxidative deamination of Gldh from *Pyrobaculum islandicum* and *Bacillus fastidiosus* were 9.7 and 8.6, respectively [41,42].

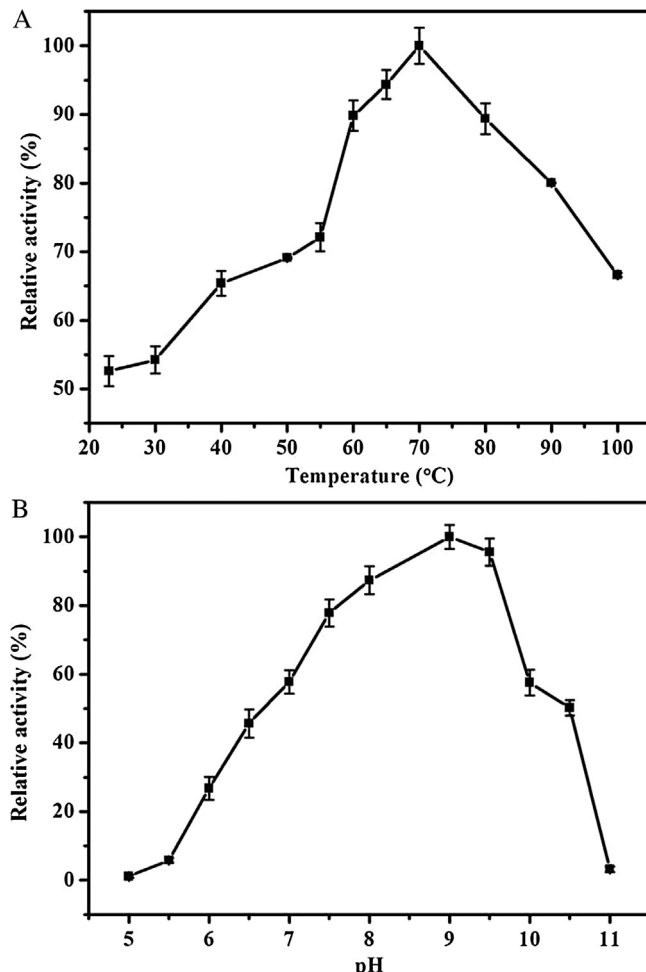
3.5. Stability of the bacteria-Gldh

As shown in Fig. 4A, for the displayed cells, Gldh could retain 70% of its original enzyme activity after being treated at 50 °C or 60 °C for 7 h, suggesting the favorable stability, which was probably originating from the decreased molecular flexibility of Gldh [43]. Like Gldh from the thermoacidophilic archaeabacterium *Sulfolobus solfataricus*, the enzyme was less stable as the temperature rose [44]. Meanwhile, a sharp drop in enzyme activity appeared as the temperature reached 80 °C, which could affect the tolerance of strain toward high temperature. It could keep more than 60% of its original activity after 3 h incubation at 90 °C. In comparison with Gldh of *Halobacterium salinarum* retaining only 55% of activity after incubation of 30 min at 90 °C, our displayed Gldh is more heat-resistant [45].

It is important to select an appropriate temperature to store Gldh-displayed cells for maintaining the enzyme activity. Fig. 4B shows the enzyme activity of bacteria-Gldh varying with storage temperature. Bacteria-Gldh almost remained the original activity over a month at 4 °C, which could be considered as the optimal storage temperature. 39.4% of Gldh activity was lost after incubation for one month at 37 °C. Moreover, the whole cell could retain

Table 1Activity of different subcellular fractions of *E. coli* cells.

Plasmid	Gldh activity (U/OD ₆₀₀) ^a				
	Whole cell	Cell lysate	Outer membrane	Cytoplasm	Inner membrane
pTlnaPbN-gdh	3.12 ± 0.12	2.97 ± 0.04	2.81 ± 0.11	0.05 ± 0.008	0.03 ± 0.006
Negative control	0.02 ± 0.003	0.03 ± 0.006	0.02 ± 0.005	ND ^b	ND ^b

^a The data were shown as mean(±SD) for three repetitive measurements, where SD stands for standard deviation.^b Not detectable.**Fig. 3.** The influence of temperature (A) and pH (B) on Gldh activity. Absorbance values at 340 nm were measured at different temperatures or pH in standard reaction system by spectrophotometer. The error bars represent the standard error of three independent experiments.

over 40% of its initial activity at 60 °C for 1 month. These results demonstrated that Gldh-cell surface display system using INP as the anchoring motif had little interference on cell membrane structure, which was consistent with other similar surface display systems [30,46]. The pH stability of Gldh is shown in Fig. 4C. A sharp decline of Gldh activity appeared when pH was lower than 7 or higher than 10, which is probably arising from the disruption of its active site. Meanwhile, the enzyme activity was stable after incubation at pH 8.0–9.0 for 8 h, and most stable at pH 8.5.

3.6. Substrate specificity and coenzyme specificity

Substrate specificity of bacteria-Gldh was examined by performing assay with other amino acids instead of L-glutamate as substrate (Table 2). A strong absorbance at 340 nm was detected due to oxidative deamination catalyzed by the cell surface

Table 2
Substrate specificity of the cell-surface displaying Gldh.

Substrate ^a	Absorbance at 340 nm ^b
L-Glutamate	0.664 ± 0.013
L-Aspartic acid	0
L-Histidine	0
L-Phenylalanine	0
L-Arginine	0
L-Lysine	0
L-Tyrosine	0
L-Threonine	0
L-Serine	0
L-Methionine	0
L-Valine	0
L-Leucine	0
L-Glycine	0

^a The concentration of each substrate is 2 mM.^b The absorbance was shown as mean(±SD) for three repetitive measurements.

displayed Gldh when L-glutamine was used as the substrate. However, no absorbance at 340 nm was detected when other amino acids were present, suggesting the high specificity of the displayed Gldh to L-glutamate. In comparison, Gldh from the hyperthermophilic archaeon *Pyrobaculum calidifontis* can catalyze not only L-glutamine, but also L-norvaline, L-valine and L-leucine, indicating that our bacteria-Gldh is more selective for L-glutamate [47]. On the other hand, when bacteria-Gldh was mixed with L-ascorbic acid, acetaminophen, and uric acid (each 5 mM) in the presence of NADP⁺, no absorbance at 340 nm was detected (data not shown), suggesting that these species have no effect on the optical detection of glutamate.

The coenzyme specificity of INP-Gldh was also detected using NADP⁺ or NAD⁺ as coenzyme, respectively. INP-Gldh exhibited catalytic activity only in the case of NADP⁺ as reducing coenzyme, which agreed with other hyperthermophilic Gdhs [47,48]. Actually, most hyperthermophilic Gldhs are NADP⁺ specific [1].

3.7. Effects of different metal ions and anions on the enzyme activity

The effects of various ions on the enzyme activity are listed in Table 3. The surface displayed Gldh in the presence of Na⁺ and K⁺ (each 100 mM) exhibited little fluctuation on activity, which is similar to Gldh from *Pyrobaculum calidifontis* [47]. Compared with alkali metal ions, NH₄⁺ at 100 mM exhibited product inhibition behavior (Eq. (1)), however, it at 10 mM NH₄⁺ had little influence, which was similar to Gldh from pumpkin cotyledon [49]. Enzyme activity appeared slight increase in the presence of Ca²⁺ and Mg²⁺(each 10 mM), which is in accordance with the purified enzymes [37,47]. Zn²⁺ (10 mM) exhibited an appreciable inhibition to enzyme activity. However, other transition metal ions such as Cu²⁺, Mn²⁺, Co²⁺, and Cd²⁺ could dramatically inhibit the activity of bacteria-Gldh, and almost 50% activity was lost at their concentration of 1 mM. Surprisingly, no absorbance peak at 340 nm was detected when 1 mM Fe³⁺ was added to the enzyme solution, indicating that Fe³⁺ could cause strong inhibition of enzyme activity. This enzyme inhibition induced by ions was similar to

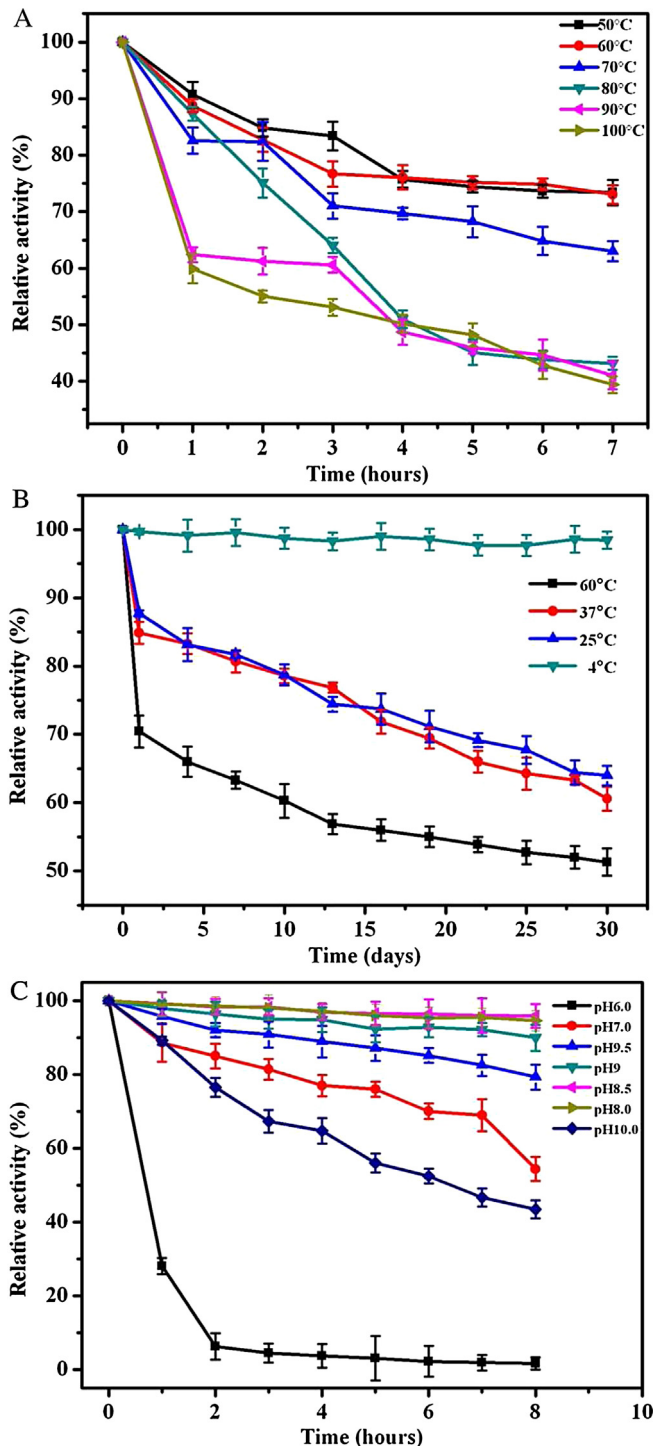


Fig. 4. (A) Thermal stability of surface displayed Gldh. (B) Effect of storage temperature on enzyme activity. (C) pH stability of surface displayed Gldh. All assays were conducted in standard system and all results were acquired from at least three independent measurements. The error bars represent the standard error of independent experiments.

alpha-amylase from *Aspergillus flavus* [50]. Actually, effect of metal ions on enzyme is a very complex issue relating to the enzyme structure and catalytic mechanism [51,52]. In addition, the common anions such as Cl^- , SO_4^{2-} , NO_3^- , Ac^- , HCO_3^- , CO_3^{2-} , H_2PO_4^- and HPO_4^{2-} (each 100 mM) had little adverse effect on the enzyme activity, probably because they do not affect the active sites of the enzyme [51].

Table 3
Effects of common ions on the enzyme activity of bacteria-Gldh.

Ion species (Conc)	Relative activity (%)
None	100
Na^+ (100 mM)	99.48 ± 1.85
K^+ (100 mM)	99.45 ± 2.34
NH_4^+ (100 mM)	50.26 ± 2.83
NH_4^+ (50 mM)	70.37 ± 2.42
NH_4^+ (10 mM)	99.91 ± 3.02
Ca^{2+} (10 mM)	120.3 ± 2.56
Mg^{2+} (10 mM)	117.7 ± 3.60
Zn^{2+} (10 mM)	72.10 ± 2.03
Cu^{2+} (1 mM)	55.08 ± 1.98
Mn^{2+} (1 mM)	51.25 ± 2.34
Co^{2+} (1 mM)	42.41 ± 3.24
Cd^{2+} (1 mM)	41.27 ± 2.02
Fe^{3+} (1 mM)	0
CO_3^{2-} (100 mM)	100.9 ± 2.15
H_2PO_4^- (100 mM)	99.95 ± 2.55
HPO_4^{2-} (100 mM)	99.92 ± 3.23
HCO_3^- (100 mM)	99.86 ± 3.01
NO_3^- (100 mM)	99.83 ± 2.32
Cl^- (100 mM)	99.62 ± 2.44
Ac^- (100 mM)	99.46 ± 2.16
SO_4^{2-} (100 mM)	99.72 ± 2.34

3.8. Detection of glutamate using cell-surface expressed Gldh

As shown in Eq. (1), glutamate is oxidized to α -ketoglutarate by Gldh in the aid of coenzyme of NADP^+ , which is then reduced to NADPH . The amount of resultant NADPH is directly proportional to the concentration of the glutamate. As addressed before, NADPH exhibits typical absorption peak at 340 nm. For different concentrations of L-glutamate in the reaction system, absorbances at 340 nm were measured using spectrophotometer. The response of substrate in the absence of any recombinant enzyme was recorded as a control. The calibration curve was obtained by plotting the absorbance at 340 nm against the L-glutamate concentration (Fig. 5). Clearly, the absorbance response was linear with concentration of L-glutamate within 10–400 μM . The limit of detection (LOD) our method was 6 μM L-glutamate ($S/N = 3$). In the context, other approaches were reported for the detection of L-glutamate with different analytical performance, for example, LODs of 68 μM and 20 μM L-glutamate were reported for polarographic biosensor and methyl viologen-modified glassy carbon electrode [19], respectively. Apparently, our approach showed better sensitivity.

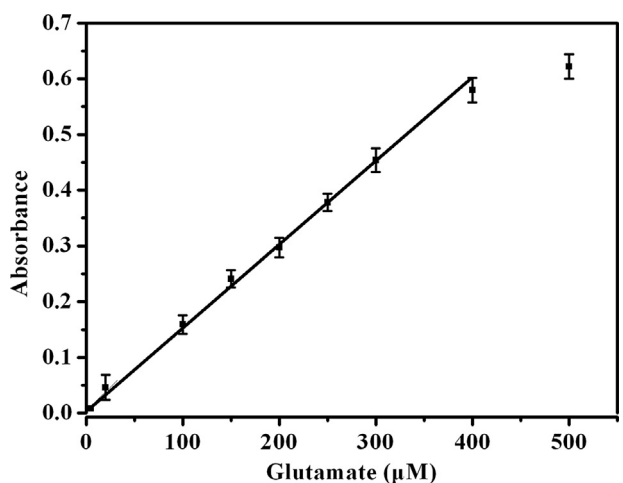


Fig. 5. The calibration curve for L-glutamate.

Table 4

Determination of L-glutamate in real samples.

Sample	L-glutamate content (w/w, %)		Relative error (%)
	This work ^a	Nutrition info	
#1 ^b	96.5 ± 3.4	99.0	-2.5
#2 ^c	77.2 ± 2.6	80.0	-3.5
#3 ^d	41.2 ± 1.0	40.0	+3.0

^a All values were shown as mean(±SD) for three repetitive measurements.^b #1 represents the local MSG.^c #2 represents the salted MSG.^d #3 represents the local chicken essence seasoning.

3.9. Detection of glutamate in real samples

To study the practicality of the developed method, the content of L-glutamate in different local flavoring agents was detected. Based on the proposed method, the samples were initially dissolved in water, followed by filtered through a 0.22-μm membrane, and the filtrates were collected and diluted with 100 mM Tris-HCl buffer (pH 8.0) solution before measurement. The results were shown in Table 4, which are in good agreement with that labeled values in the Nutritional Information on the package, demonstrating that the recombinant cells were capable of precise detection of L-glutamate.

4. Conclusions

In summary, Gldh was first to successfully display on the cell surface of *E. coli* using inaPb from *P. borealis* as an anchoring motif. The fusion protein was about 60 kDa, which was confirmed by SDS-PAGE analysis. The majority of Gldh activity was detected in the outer membrane fraction, suggesting that the Gldh could be displayed on the cell surface in its active form. The Gldh surface displayed cells showed high activity under the optimal pH and temperature conditions. The bacteria-Gldh is NADP⁺ dependent and specific to L-glutamate, which exhibited excellent stability and ion tolerance. Finally, the oxidization of L-glutamate by the cell surface displayed Gldh with NADP⁺ as cofactor was applied to develop optical method to detect L-glutamate. Considering all the excellent properties mentioned above, the bacteria-Gldh holds great potential as biocatalyst for biosensor and industrial catalysis applications.

Acknowledgements

This work was supported in part by National Natural Science Foundation of China (Nos. 91227116, 31200598, 21275152, 31300663 and 21475144) and the Qingdao Institute of Bioenergy and Bioprocess Technology Director Innovation Foundation for Young Scientists (Y37203210S).

References

- Hudson RC, Daniel RM. L-glutamate dehydrogenases: distribution, properties and mechanism. *Comp Biochem Physiol B: Biochem Mol Biol* 1993;106:767–92.
- Commichau FM, Gunka K, Landmann JJ, Stulke J. Glutamate metabolism in *Bacillus subtilis*: gene expression and enzyme activities evolved to avoid futile cycles and to allow rapid responses to perturbations of the system. *J Bacteriol* 2008;190:3557–64.
- Choi DW. Glutamate neurotoxicity and diseases of the nervous system. *Neuron* 1988;1:623–34.
- Owen OE, Kalhan SC, Hanson RW. The key role of anaplerosis and cataplerosis for citric acid cycle function. *J Biol Chem* 2002;277:30409–12.
- Obrenovitch TP, Urenjak J, Zilkha E, Jay TM. Excitotoxicity in neurological disorders—the glutamate paradox. *Int J Dev Neurosci* 2000;18:281–7.
- Hasell AS. Excitotoxic mechanisms in stroke: an update of concepts and treatment strategies. *Neurochem Int* 2007;50:941–53.
- Sheldon AL, Robinson MB. The role of glutamate transporters in neurodegenerative diseases and potential opportunities for intervention. *Neurochem Int* 2007;51:333–55.
- Yu Y, Sun Q, Zhou T, Zhu M, Jin L, Shi G. On-line microdialysis system with poly(amidoamine)-encapsulated Pt nanoparticles biosensor for glutamate sensing in vivo. *Bioelectrochemistry* 2011;81:53–7.
- Vyas CA, Rawls SM, Raffa RB, Shackman JC. Glutamate and aspartate measurements in individual planaria by rapid capillary electrophoresis. *J Pharmacol Toxicol Methods* 2011;63:119–22.
- Bonizzoni M, Fabbrioli L, Piovani G, Taglietti A. Fluorescent detection of glutamate with a dicopper(II) polyamine cage. *Tetrahedron* 2004;60:11159–62.
- Eckstein JA, Ammerman GM, Reveles JM, Ackermann BL. Analysis of glutamine, glutamate, pyroglutamate, and GABA in cerebrospinal fluid using ion pairing HPLC with positive electrospray LC/MS/MS. *J Neurosci Methods* 2008;171:190–6.
- Spreux-Varoquaux O, Bensimon G, Lacomblez L, Salachas F, Pradat PF, Le Forestier N, et al. Glutamate levels in cerebrospinal fluid in amyotrophic lateral sclerosis: a reappraisal using a new HPLC method with coulometric detection in a large cohort of patients. *J Neurol Sci* 2002;193:73–8.
- Clarke G, O'Mahony S, Malone G, Dinan TG. An isocratic high performance liquid chromatography method for the determination of GABA and glutamate in discrete regions of the rodent brain. *J Neurosci Methods* 2007;160:223–30.
- Shah AJ, de la Flor R, Atkins A, Slone-Murphy J, Dawson LA. Development and application of a liquid chromatography/tandem mass spectrometric assay for measurement of N-acetylaspartate, N-acetylaspartylglutamate and glutamate in brain slice superfusates and tissue extracts. *J Chromatogr B* 2008;876:153–8.
- Khampha W, Meevootisom V, Wiyakrupta S. Spectrophotometric enzymatic cycling method using L-glutamate dehydrogenase and D-phenylglycine aminotransferase for determination of L-glutamate in foods. *Anal Chim Acta* 2004;520:133–9.
- Batra B, Kumari S, Pundir CS. Construction of glutamate biosensor based on covalent immobilization of glutamate oxidase on polypyrrole nanoparticles/polyaniline modified gold electrode. *Enzyme Microb Technol* 2014;57:69–77.
- Özel RE, Ispas C, Ganesana M, Leiter JC, Andreeșu S. Glutamate oxidase biosensor based on mixed ceria and titania nanoparticles for the detection of glutamate in hypoxic environments. *Biosens Bioelectron* 2014;52:397–402.
- Kergoat L, Piro B, Simon DT, Pham M-C, Noël V, Berggren M. Detection of glutamate and acetylcholine with organic electrochemical transistors based on conducting polymer/platinum nanoparticle composites. *Adv Mater* 2014;26:5658–64.
- Maalouf R, Chebib H, Saïkali Y, Vittori O, Sigaud M, Jaffrezic-Renault N. Amperometric and impedimetric characterization of a glutamate biosensor based on Nafion® and a methyl viologen modified glassy carbon electrode. *Biosens Bioelectron* 2007;22:2682–8.
- Lee SY, Choi JH, Xu Z. Microbial cell-surface display. *Trends Biotechnol* 2003;21:45–52.
- Kondo A, Ueda M. Yeast cell-surface display—applications of molecular display. *Appl Microbiol Biotechnol* 2004;64:28–40.
- Jung H-C, Lebeault J-M, Pan J-G. Surface display of *Zymomonas mobilis* levansucrase by using the ice-nucleation protein of *Pseudomonas syringae*. *Nat Biotechnol* 1998;16:576–80.
- Yang TH, Pan JG, Seo YS, Rhee JS. Use of *pseudomonas putida* EstA as an anchoring motif for display of a periplasmic enzyme on the surface of *Escherichia coli*. *Appl Environ Microbiol* 2004;70:6968–76.
- Shiraga S, Kawakami M, Ishiguro M, Ueda M. Enhanced reactivity of *Rhizopus oryzae* lipase displayed on yeast cell surfaces in organic solvents: potential as a whole-cell biocatalyst in organic solvents. *Appl Environ Microbiol* 2005;71:4335–8.
- Lee SH, Choi JI, Park SJ, Lee SY, Park BC. Display of bacterial lipase on the *Escherichia coli* cell surface by using FadL as an anchoring motif and use of the enzyme in enantioselective biocatalysis. *Appl Environ Microbiol* 2004;70:5074–80.
- Xu Z, Lee SY. Display of polyhistidine peptides on the *Escherichia coli* cell surface by using outer membrane protein C as an anchoring motif. *Appl Environ Microbiol* 1999;65:5142–7.
- Fujita Y, Katahira S, Ueda M, Tanaka A, Okada H, Morikawa Y, et al. Construction of whole-cell biocatalyst for xylan degradation through cell-surface xylanase display in *Saccharomyces cerevisiae*. *J Mol Catal B: Enzym* 2002;17:189–95.
- Fukuda T, Tsuchiyama K, Makishima H, Takayama K, Mulchandani A, Kuroda K, et al. Improvement in organophosphorus hydrolase activity of cell surface-engineered yeast strain using Flo1p anchor system. *Biotechnol Lett* 2010;32:655–9.
- Liang B, Li L, Mascini M, Liu A. Construction of xylose dehydrogenase displayed on the surface of bacteria using ice nucleation protein for sensitive xylose detection. *Anal Chem* 2012;84:275–82.
- Liang B, Li L, Tang X, Lang Q, Wang H, Li F, et al. Microbial surface display of glucose dehydrogenase for amperometric glucose biosensor. *Biosens Bioelectron* 2013;45:19–24.
- Tang X, Liang B, Yi T, Manco G, Palchetti I, Liu A. Cell surface display of organophosphorus hydrolase for sensitive spectrophotometric detection of p-nitrophenol substituted organophosphates. *Enzyme Microb Technol* 2014;55:107–12.
- Tang X, Zhang T, Liang B, Han D, Zeng L, Zheng C, et al. Sensitive electrochemical microbial biosensor for p-nitrophenylorganophosphates based on electrode modified with cell surface-displayed organophosphorus hydrolase and ordered mesoporous carbons. *Biosens Bioelectron* 2014;60:137–42.
- Li L, Liang B, Shi JG, Li F, Mascini M, Liu AH. A selective and sensitive D-xylose electrochemical biosensor based on xylose dehydrogenase displayed on the

- surface of bacteria and multi-walled carbon nanotubes modified electrode. *Biosens Bioelectron* 2012;33:100–5.
- [34] Li L, Liang B, Li F, Shi JG, Mascini M, Lang QL, et al. Co-immobilization of glucose oxidase and xylose dehydrogenase displayed whole cell on multiwalled carbon nanotube nanocomposite films modified-electrode for simultaneous voltammetric detection of D-glucose and D-xylose. *Biosens Bioelectron* 2013;42:156–62.
- [35] Xia L, Liang B, Li L, Tang XJ, Palchetti I, Mascini M, et al. Direct energy conversion from xylose using xylose dehydrogenase surface displayed bacteria based enzymatic biofuel cell. *Biosens Bioelectron* 2013;44:160–3.
- [36] Hou C, Yang D, Liang B, Liu A. Enhanced performance of glucose/O₂ biofuel cell assembled with laccase-covalently immobilized three-dimensional macroporous gold film based biocathode. *Anal Chem* 2014;86:6057–63.
- [37] Lee M-K, González JM, Robb FT. Extremely thermostable glutamate dehydrogenase (GDH) from the freshwater archaeon *Thermococcus waiotapuensis*: cloning and comparison with two marine hyperthermophilic GDHs. *Extremophiles* 2002;6:151–9.
- [38] Lowry OH, Passonneau JV, Rock MK. The stability of pyridine nucleotides. *J Biol Chem* 1961;236:2756–9.
- [39] Sakamoto N, Kotre AM, Savageau MA. Glutamate dehydrogenase from *Escherichia coli*: purification and properties. *J Bacteriol* 1975;124:775–83.
- [40] Ertan H. Some properties of glutamate dehydrogenase, glutamine synthetase and glutamate synthase from *Corynebacterium callunae*. *Arch Microbiol* 1992;158:35–41.
- [41] Kujo C, Ohshima T. Enzymological characteristics of the hyperthermostable NAD-dependent glutamate dehydrogenase from the archaeon *Pyrobaculum islandicum* and effects of denaturants and organic solvents. *Appl Environ Microbiol* 1998;64:2152–7.
- [42] Op Den Camp HJM, Liem KD, Meesters P, Hermans JMH, Van Der Drift C. Purification and characterization of the NADP-dependent glutamate dehydrogenase from *Bacillus fastidiosus*. *Antonie van Leeuwenhoek* 1989;55:303–11.
- [43] Viñinen M. Relationship of protein flexibility to thermostability. *Protein Eng* 1987;1:477–80.
- [44] Consalvi V, Chiaraluce R, Politi L, Gambacorta A, De Rosa M, Scandurra R. Glutamate dehydrogenase from the thermoacidophilic archaebacterium *Sulfolobus solfataricus*. *Eur J Biochem* 1991;196:459–67.
- [45] Munawar N, Engel PC. Overexpression in a non-native halophilic host and biotechnological potential of NAD super(+) -dependent glutamate dehydrogenase from *Halobacterium salinarum* strain NRC-36014. *Extremophiles* 2012;16:463–76.
- [46] Liang B, Lang Q, Tang X, Liu A. Simultaneously improving stability and specificity of cell surface displayed glucose dehydrogenase mutants to construct whole-cell biocatalyst for glucose biosensor application. *Bioresour Technol* 2013;147:492–8.
- [47] Wakamatsu T, Higashi C, Ohmori T, Doi K, Ohshima T. Biochemical characterization of two glutamate dehydrogenases with different cofactor specificities from a hyperthermophilic archaeon *Pyrobaculum calidifontis*. *Extremophiles* 2013;17:379–89.
- [48] Alén N, Steen IH, Birkeland N-K, Lien T. Purification and properties of an extremely thermostable NADP⁺-specific glutamate dehydrogenase from *Archaeoglobus fulgidus*. *Arch Microbiol* 1997;168:536–9.
- [49] Chou KH, Splittstoesser WE. Glutamate dehydrogenase from pumpkin cotyledons characterization and isoenzymes. *Plant Physiol* 1972;49: 550–4.
- [50] Abou-Zeid A. Production, purification and characterization of an extracellular alpha-amylase enzyme isolated from *Aspergillus flavus*. *Microbios* 1997;89:55–66.
- [51] Zhao H. Effect of ions and other compatible solutes on enzyme activity, and its implication for biocatalysis using ionic liquids. *J Mol Catal B: Enzym* 2005;37:16–25.
- [52] Lerner AB. Mammalian tyrosinase: effect of ions on enzyme action. *Arch Biochem Biophys* 1952;36:473–81.